Constrained MPC Design for Heave Disturbance Attenuation in Offshore Drilling Systems

Amirhossein Nikoofard*, Tor Arne Johansen, Hessam Mahdianfar, and Alexey Pavlov

***Abstract*—This paper presents a constrained model predictive control scheme for regulation of the annular pressure in a well during managed pressure drilling from a floating rig subject to heave motion. The results show that closed-loop simulation without disturbance has a fast regulation response and without any overshoot. The robustness of controller to deal with heave disturbances is investigated. The constrained MPC shows good disturbance rejection capabilities. The simulation results show that this controller has better performance than a PID controller and is also capable of handling constraints of the system with the heave disturbance.**

***Index Terms*—Managed pressure drilling, heave Compensation and model predictive control.**

I. Introduction

In drilling operations, a fluid called mud is pumped down through the drill string and flows through the drill bit at the bottom of the well (see Figure 1). Then the mud flows up the well annulus carrying cuttings out of the well. To avoid fracturing, collapse of the well, or influx of formation fluids surrounding the well, it is crucial to control the pressure in the open part of the annulus within a certain operating window. In conventional drilling, this is done by mixing a mud of appropriate density and adjusting mud pump flow-rates. In managed pressure drilling (MPD), the annulus is sealed and the mud exits through a controlled choke, allowing for faster and more precise control of the annular pressure. In automatic MPD systems, the choke is controlled by an automatic control system which manages the annular mud pressure to be within specified upper and lower limits. Different aspects of modeling for MPD have been studied in the literature [1]–[5]. Estimation and control design in MPD has been investigated by several researchers [5]–[10], focusing mainly on pressure control during drilling from a fixed platform.

When designing MPD control systems, one should take into account various operational procedures and disturbances that affect the pressure inside the well. There is a specific disturbance occurring during drilling from floaters that significantly affects MPD operations. In this case, the rig moves vertically with the waves, referred to as heave motion. As drilling proceeds, the drill string needs to be extended with new sections. Thus, every couple of hours or so, drilling is stopped to add a new segment of about 27 meters to the drill string. During drilling, a heave compensation mechanism is active that isolates the drill string from the heave motion of the rig. However, during connections, the pump is stopped and the string is disconnected from the heave compensation mechanism and rigidly connected to the rig. The drill string then moves vertically with the heave motion of the floating rig, and acts like a piston on the mud in the well. The heave motion may be more than 3 meters in amplitude and typically has a period of 10-20 seconds, which causes a severe pressure fluctuations at the bottom of the well. Pressure fluctuations have been observed to be an order of magnitude higher than the standard limits for pressure regulation accuracy in MPD, which is about ± 2.5 bar. Downward movement of the drill string into the well increases pressure(surging), and upward

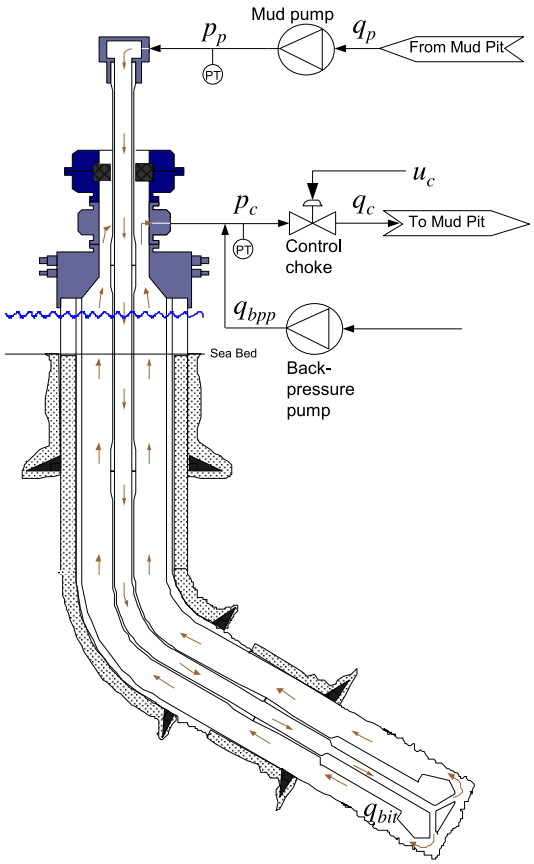

Figure 1. Schematic of an MPD system (Courtesy of Glenn-Ole Kaasa, Statoil Research Centre.)

Amirhossein Nikoofard, Tor Arne Johansen and Hessam Mahdianfar are with the Center for Autonomous Marine Operations and Systems (AMOS), Department of Engineering Cybernetics, Norwegian University of Science and Technology, Trondheim, Norway.

Alexey Pavlov is a principal researcher at Statoil Research Centre, Department of Intelligent Well Construction, Porsgrunn, 3910, Norway.

*Corresponding author :
amirhossein.nikoofard@itk.ntnu.no

movement decreases pressure (swabbing). Excessive surge and swab pressures can lead to mud loss resulting from high pressure fracturing the formation or a kick-sequence (uncontrolled influx from the reservoir) that can potentially grow into a blowout as a consequence of low pressure.

Rasmussen et al. [11], compared and evaluated different MPD methods for compensation of surge and swab pressure. Pavlov et al. [12], presented two nonlinear control algorithms for handling heave disturbances in MPD operations. Mahdianfar et al. [13], [14], designed an infinite-dimensional observer that estimates the heave disturbance. This estimation is used in a controller to reject the effect of the disturbance on the down-hole pressure.

Model predictive control (MPC) is one of the popular controllers for complex constrained multivariable control problem in industry and has been the subject of many studies since the 1970s (e.g. see [15]–[18]). At each sampling time, a MPC control action is acquired by the on-line solution of a finite horizon open-loop optimal control problem. Although more than one control action is obtained, only the first one is implemented to the plant. At the next sampling time, the computation is repeated with new measurements obtained from the system. The purpose of this paper is to design a constrained MPC scheme for controlling the pressure during MPD oil well drilling. One of the criteria for evaluating the controller performance is its ability to handle heave disturbances.This scheme is compared with a standard PID-control scheme.

In the following sections, a model based on mass and momentum balances that provides the governing equations for pressure and flow in the annulus is given. A stochastic modeling of waves in the North Sea is used and heave disturbance induced by elevation motion of sea surface is modeled. The design of a constrained MPC scheme is presented and applied on Managed Pressure Drilling to show that this controller has robust performance with a comparison with PID controller.

II. Mathematical Modeling

A. Annulus flow dynamics

The governing equations for flow in an annulus is derived from mass and momentum balances [2]

$$\frac{\partial p}{\partial t} = -\frac{\beta}{A}\frac{\partial q}{\partial x} \tag{1}$$

$$\frac{\partial q}{\partial t} = -\frac{A}{\rho_0}\frac{\partial p}{\partial x} - \frac{F}{\rho_0} + Ag\cos(\alpha(x)) \tag{2}$$

where $p(x,t)$ and $q(x,t)$ are the pressure and volumetric flow rate at location x and time t, respectively. The bulk modulus of the mud is denoted by β. $A(x)$ is the cross section area, ρ is the (constant) mass density, F is the friction force per unit length, g is the gravitational constant and $\alpha(x)$ is the angle between gravity and the positive flow direction at location x in the well (Figure 2). To derive a set of ordinary differential equations describing the dynamics of the pressures and flows at different positions in the well, equations (1) and (2) are discretized by using a finite volumes method. To solve this problem, the annulus is divided into a number of control volumes, as shown in Figure 2, and integrating (1) and (2) over each control volume.

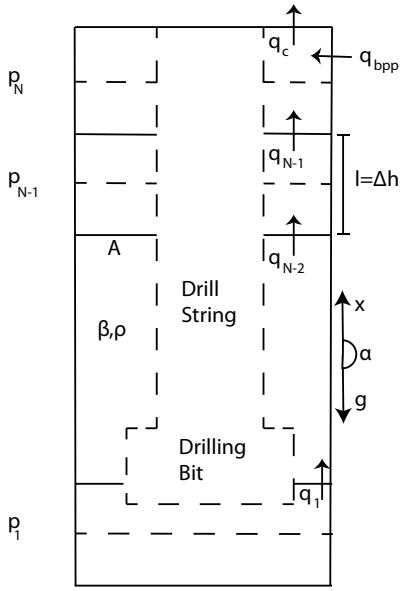

Figure 2. Control volumes of annulus hydraulic model [2]

Landent et al. found that [2] a five control volumes model could capture the main dynamics of the system in case of heave disturbance for a well from Ullrigg[1] test facility with a particular length of about 2000m and with water based mud. We will use parameters corresponding to that well as a base case throughout the paper. The set of nine ordinary differential equations describing five control volumes in the annulus are as follows [1] and [19]

$$\dot{p}_1 = \frac{\beta_1}{A_1 l_1}(-q_1 - v_d A_d) \tag{3}$$

$$\dot{p}_2 = \frac{\beta_2}{A_2 l_2}(q_1 - q_2) \tag{4}$$

$$\dot{p}_3 = \frac{\beta_3}{A_3 l_3}(q_2 - q_3) \tag{5}$$

$$\dot{p}_4 = \frac{\beta_4}{A_4 l_4}(q_3 - q_4) \tag{6}$$

$$\dot{p}_5 = \frac{\beta_5}{A_5 l_5}(q_4 - q_c + q_{bpp}) \tag{7}$$

$$\dot{q}_i = \frac{A_i}{l_i \rho_i}(p_i - p_{i+1}) - \frac{F_i(q_i)A_i}{l_i \rho_i} - A_i g \frac{\Delta h_i}{l_i} \tag{8}$$

$$q_c = K_c\sqrt{p_c - p_0}G(u) \tag{9}$$

where, $i = 1, ..., 4$, and the numbers $1, ..., 5$ refer to control volume number, with 1 being the lower most control volume representing the down hole pressure ($p_1 = p_{bit}$), and 5 being the upper most volume representing the choke pressure

[1]Ullrigg is a full scale drilling test facility located at International Research Institute of Stavanger (IRIS).

($p_5 = p_c$). v_d is the heave vertical velocity due to ocean waves. The length of each control volume is denoted by l, and the height difference is Δh. Notice since the well may be non-vertical, l_i and Δh_i may in general differ from each other. The means for pressure control are the back pressure pump flow q_{bpp} and the choke flow q_c. The flow from the back pressure pump q_{bpp} is linearly related to the pump frequency and cannot be changed fast enough to compensate for the heave-induced pressure fluctuations. Therefore, it is the choke flow that is used primarily for control, which is modeled by nonlinear orifice equation. K_c is the choke constant corresponding to the area of the choke and the density of the drilling fluid. p_0 is the (atmospheric) pressure downstream the choke and $G(u)$ is a strictly increasing and invertible function relating the control signal to the actual choke opening, taking its values on the interval $[0, 1]$.

Based on experimental results from full scale tests at Ullrigg, the friction force in the annulus is considered to be a linear function of the flow rate [2]. Friction force on the i^{th} control volume is

$$F_i(q_i) = \frac{k_{fric} q_i}{A_i} \tag{10}$$

where k_{fric} is constant (or, more likely, slowly varying) friction coefficient.

B. Waves Response Modeling

Environmental forces due to waves, wind and ocean currents are considered disturbances to the motion control system of floating vessels. These forces, which can be described in stochastic terms, are conceptually separated into low-frequency (LF) and wave-frequency (WF) components, [20].

Ocean waves are random in terms of both time and space. Therefore, a stochastic modeling description seems to be the most appropriate approach to describe them. The model presented in this part is for purposes of controller design and verification. For control system design it is common to assume the principle of superposition when considering wind and wave disturbances. For most marine control applications this is a good approximation [20].

During normal drilling operations the WF part of the drill-string motion is compensated for by the heave control system, [21]–[23]. However, during connections the drill-string is disconnected from the heave compensation mechanism and rigidly connected to the rig. Thus, it moves vertically with the heave motion of the floating rig, and causes severe down-hole pressure fluctuations.

1) Linear Approximation for WF Position: When simulating and testing feedback control systems, it is useful to have a simple and effective way of representing the wave forces. Here the motion Response Amplitude Operators (RAO) are represented as a state-space model where the wave spectrum is approximated by a linear filter. In this setting RAO vessel model is represented in Figure 3,where $H_{rao}(s)$ is the wave amplitude-to-force transfer function and $H_v(s)$ is the force-to-motion transfer function. In addition to this, the response of the motion RAOs and the linear vessel dynamics in cascade is modeled as constant tunable gains, [20]:

$$\boldsymbol{K} = \text{diag}\{K^1, K^2, K^3, K^4, K^5, K^6\} \tag{11}$$

This means that the RAO vessel model is approximated as (Figure 3)

$$H_{rao}(s) H_v(s) \approx K \tag{12}$$

The fixed-gain approximation (equation 12) produces good results in a closed-loop system where the purpose is to test robustness and performance of a feedback control system in the presence of waves.

Figure 3. Linear approximation for computation of wave-induced positions.

If the fixed gain approximation (equation 12) is applied, the generalized WF position vector η_w in Figure 3 becomes

$$\eta_w = K H_s(s) w(s) \tag{13}$$

where $H_s(s)$ is a diagonal matrix containing linear approximations of the wave spectrum $S(\omega)$. The WF position for the degree of freedom related to heave motion becomes

$$\eta_w^h = K^h \xi^h \tag{14}$$

$$\xi^h(s) = h^h(s) w^h(s) \tag{15}$$

where $h^h(s)$ is a linear approximation of the wave spectral density function $S(\omega)$ and $w^h(s)$ is a zero-mean Gaussian white noise process with unity power across the spectrum:

$$P_{ww}^h(\omega) = 1.0 \tag{16}$$

Hence, the power spectral density (PSD) function for $\xi^h(s)$ can be computed as

$$P_{\xi\xi}^h(\omega) = |h^h(j\omega)|^2 P_{ww}^h(\omega) = |h^h(j\omega)|^2 \tag{17}$$

Here we approximate $S(\omega)$ with $P_{\xi\xi}^h(\omega)$, for instance by means of nonlinear regression, such that $P_{\xi\xi}^h(\omega)$ reflects the power distribution of $S(\omega)$ in the relevant frequency range.

2) JONSWAP Spectrum: The JONSWAP spectrum is representative for wind-generated waves under the assumption of finite water depth and limited fetch, [20], [24]. The spectral density function is written

$$S(\omega) = 155 \frac{H_s^2}{T_1^4} \omega^{-5} \exp\left(\frac{-944}{T_1^4} \omega^{-4}\right) \gamma^Y \tag{18}$$

where H_s is the significant wave height, T_1 is the average wave period, $\gamma = 3.3$ and

$$Y = \exp\left[-\left(\frac{0.191\omega T_1 - 1}{\sqrt{2}\sigma}\right)^2\right] \tag{19}$$

where

$$\sigma = \begin{cases} 0.07 & \text{for } \omega \leq 5.24/T_1 \\ 0.09 & \text{for } \omega > 5.24/T_1 \end{cases} \tag{20}$$

The modal period, T_0, is related to the average wave period through $T_1 = 0.834\,T_0$, [20].

Figure 4, produced using MSS Toolbox[2], shows the JONSWAP spectrum power distribution curve. The parameter values for H_s and T_0 are taken from [25]. From Figure 4 we can see that the JONSWAP spectrum is a narrow band spectrum, and its energy is mainly focused on $0.5-1.5\,rad/s$, and the peak frequency is $\omega_0 = 0.7222\,rad/s$.

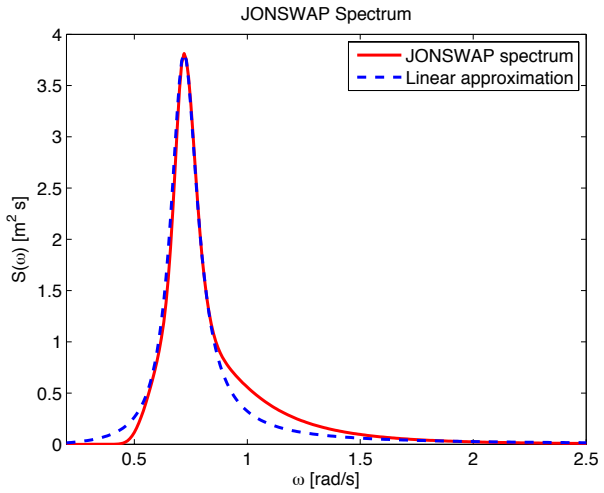

Figure 4. JONSWAP spectrum and its approximation.

3) Second-Order Wave Transfer Function Approximation: As discussed earlier a linear wave response approximation for $H_s(s)$ is usually preferred by ship control systems engineers, because of its simplicity and applicability:

$$h^h(s) = \frac{2\lambda\omega_0\sigma s}{s^2 + 2\lambda\omega_0 s + \omega_0^2} \tag{21}$$

where $\lambda = 0.1017$, $\sigma = 1.9528$, $H_s = 4.70$, $T_0 = 8.70$, $\omega_0 = 0.7222$ are typical parametrs. The transfer function approximation is shown in Figure 4.

III. Controller Design

The model described by equations (3)-(9) is in form of a nonlinear strict feedback system, with an unmatched stochastic disturbance. By considering $a_j = \frac{\beta_j}{A_j l_j}$, $b_j = \frac{A_j}{l_j \rho_j}$, $c_j = \frac{K_{fric}}{\rho_j l_j}$, the model in state-space form would be

$$\begin{cases} \dot{X} = AX + Bu_a + B_1 + Ed \\ y = CX \end{cases} \tag{22}$$

[2]MSS. Marine Systems Simulator (2010), version 3.3. Viewed 26.03.2011, http://www.marinecontrol.org.

where

$$X = \begin{bmatrix} p_1 & q_1 & p_2 & q_2 & p_3 & q_3 & p_4 & q_4 & p_5 \end{bmatrix}^T$$

$$A = \begin{bmatrix} 0 & -a_1 & 0 & 0 & 0 & 0 & 0 & 0 & 0 \\ b_1 & -c_1 & -b_1 & 0 & 0 & 0 & 0 & 0 & 0 \\ 0 & a_2 & 0 & -a_2 & 0 & 0 & 0 & 0 & 0 \\ 0 & 0 & b_2 & -c_2 & -b_2 & 0 & 0 & 0 & 0 \\ 0 & 0 & 0 & a_3 & 0 & -a_3 & 0 & 0 & 0 \\ 0 & 0 & 0 & 0 & b_3 & -c_3 & -b_3 & 0 & 0 \\ 0 & 0 & 0 & 0 & 0 & a_4 & 0 & -a_4 & 0 \\ 0 & 0 & 0 & 0 & 0 & 0 & b_4 & -c_4 & -b_4 \\ 0 & 0 & 0 & 0 & 0 & 0 & 0 & a_5 & 0 \end{bmatrix}$$

$$B = \begin{bmatrix} 0 & 0 & 0 & 0 & 0 & 0 & 0 & 0 & a \end{bmatrix}^T$$

$$B_1 = -263.7814 \begin{bmatrix} 0 & 1 & 0 & 1 & 0 & 1 & 0 & 1 & 0 \end{bmatrix}^T$$

$$E = \begin{bmatrix} -22.0857 & 0 & 0 & 0 & 0 & 0 & 0 & 0 & 0 \end{bmatrix}^T$$

$$C = \begin{bmatrix} 1 & 0 & 0 & 0 & 0 & 0 & 0 & 0 & 0 \end{bmatrix} \tag{23}$$

and

$$u_a = q_{bpp} - q_c \tag{24}$$

The heave disturbance v_d in equation (3) will be compensated by using constrained MPC designed in the next part. Note that the hydrostatic pressures in equation (8) are included in the states p_i in (3)-(7). $p_1 = p_{bit}$ is the output of the process.

A. Constrained MPC design

Consider the discrete-time linear time-invariant input-affine system

$$\begin{cases} x(k+1) = Ax(k) + Bu(k) + B_1 + Ed(k) \\ y(k) = Cx(k), \end{cases} \tag{25}$$

while fulfilling the constraints

$$y_{min} \le y(k) \le y_{max}, \;\; u_{min} \le u(k) \le u_{max} \tag{26}$$

at all time instants $k \ge 0$.
In (25)-(26), n , p and m are the number of states, outputs and inputs respectively, and $x(k) \in \Re^n$, $y(k) \in \Re^p$, $d(k) \in \Re^n$ and $u(k) \in \Re^m$ are the state, output, disturbance and input vectors respectively.
The constrained MPC solves a constrained optimal regulation problem at each time k. The following optimization problem

$$\begin{aligned} \underset{U \triangleq \{u_k, \cdots, u_{k+N}\}}{min} \;\; & \{J(u,y,r) = \sum_{i=1}^{N} [(u(k+i|k)^T R u(k+i|k) + \\ & (y(k+i|k) - r(k+i|k))^T Q (y(k+i|k) - r(k+i|k))]\} \end{aligned}$$

$$\begin{aligned} s.t \quad & y_{min} \le y_{i+k|k} \le y_{max} \quad i = 1, \cdots, N, \\ & u_{min} \le u_{t+k|k} \le y_{max} \quad i = 1, \cdots, N, \\ & x_{k|k} = x(k) \\ & x_{i+k+1|k} = Ax_{i+k|k} + Bu_{i+k|k} + B_1 + Ed_{i+k|k}, \\ & y_{i+k|k} = Cx_{i+k|k} \end{aligned} \tag{27}$$

is solved on-line at each sample time, where N, J and r are the finite horizon, cost function and reference trajectory

respectively, the subscript "$(k+i|k)$" denotes the value predicted for time $k+i$, we assume that Q and R are the positive definite matrices.
As the states $x(k)$ is not directly measurable, prediction are computed from estimation of states. The state observer is designed to provide estimation of states $x(k)$, since the pair (C, A) is detectable. The controller computes the optimal solution U by solving the quadratic programing (QP). If the future value of disturbances and/or measurement of disturbances are not known then disturbances are assumed to be zero in MPC predictions.

Controller parameters such as weight of inputs, inputs rate and outputs and control horizon must be tuned to achieve the good performance and stability in this problem. The prediction horizon should be tuned properly to ensure the closed-loop stability of the control system.

IV. Simulation Results

The parameters for simulations, identified from the IRIS-Drill simulator, are given in Table I.

Table I
Parameter Values

Parameter	Value	Parameter	Value
a	$2.254 \times 10^8\ [Pa/m^3]$	g	$9.806\ [m/s^2]$
b	$4.276 \times 10^{-8}\ [m^4/Kg]$	A	$0.0269\ [m^2]$
K_f	$5.725 \times 10^5\ [sPa/m^3]$	e	$0.2638\ [m^3/s^2]$
c	$14.4982\ [1/sm^2]$	A_d	$0.0291\ [m^2]$
K_G	0.0650	K_c	2.32
q_{bpp}	$369.2464\ [m^3/s]$	p_0	$101325\ [pa]$

The time-step used for discretizing the dynamic optimization model was 0.1 s. The input weight (R), input rate weight ($R_{\delta u}$), output weight (Q) and prediction horizon (N) are chosen 150, 0, 17 and 100 respectively. In this problem, prediction horizon is set large compared with the settling time to ensure the closed-loop stability of the control system. The weights specify trade-offs in the controller design. Choosing larger output weight or smaller input weight results in overshoot in closed-loop response and sometimes broken constraints. In other words, if you choose larger input weight or smaller output weight then the closed loop response is slower or sometimes unstable.

To compare the impact of MPC on the drilling system with other controllers, a PID controller was applied to the system as well. A PID controller is chosen due to its popularity in the industry. Proportional, integral and derivative gain are chosen 0.75, 0.002 and -1 respectively. The Bode plot of the loop transfer function with the PID is shown in Figure 5. Bandwidth with PID is less than 1.3 rad/sec, and the phase drops very quickly. So, it is not realistic to get a bandwidth of about 5 rad/sec which would be desirable for this disturbance.

Three different simulations are performed. The first simulation is shown in Figures 6 and 7, where the nominal

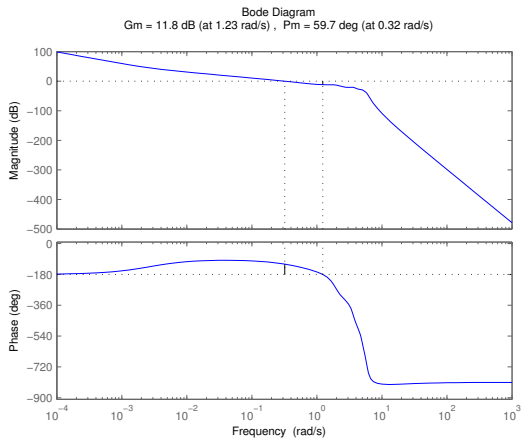

Figure 5. Bode plot of the loop transfer function with the PID.

model is used for generating the measurements. A soft constraint of 2.5bar (compared to the reference pressure) and a constraint of choke opening taking its values on the interval $[0, 1]$ are included in the constrained MPC optimization. Figure 6 compares the responses of the PID controller and constrained MPC to regulate set point trajectory. In the proposed MPC controller, the bottom-hole pressure approaches to set point fast without any overshoot. In comparison to MPC controller, PID controller has some overshoot and somewhat slower response. The choke control signal in constrained MPC is illustrated in Figure 7.

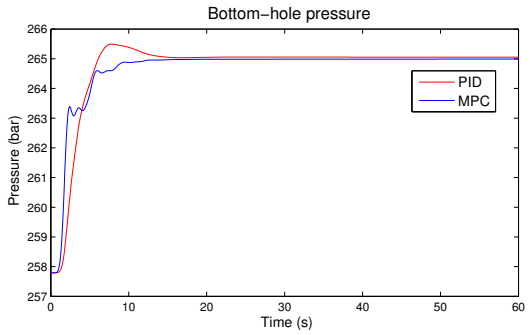

Figure 6. Bottom-hole pressure without disturbance.

The second simulation is shown in Figures 8, 9 and 10, where the nominal model with heave disturbance is used for generating the measurements. The same constraints as in previous simulation are enforced to the controller. Figure 8 compares the responses of constant input ($q_{bpp} = q_c$) and constrained MPC to track the set point reference with existing heave disturbance. A constant input couldn't reduce the effect of heave disturbance and track the set point reference. Figure 9 compares the responses of PID controller and constrained MPC to track the set point reference with a heave disturbance. It is found that the MPC controller is capable of maintaining the constraints whereas the PID controller is not. The choke

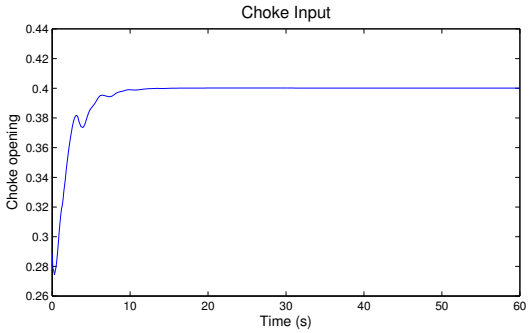

Figure 7. MPC control signal to the choke without disturbance.

control signal is illustrated in Figure 10. As indicated in this figure, the constrained MPC shows good disturbance rejection capabilities. Figure 11 shows heave disturbance pressure variations.

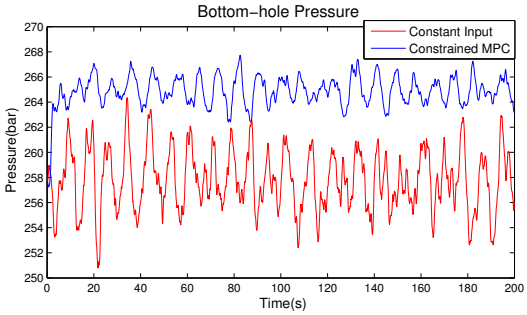

Figure 8. Bottom-hole pressure

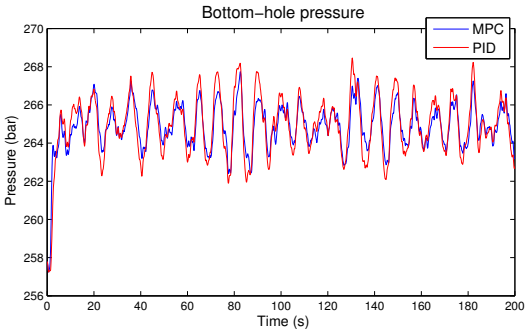

Figure 9. Bottom-hole pressure with heave disturbance.

The last simulation is shown in Figure 12 where the nominal model with heave disturbance is used for generating the measurements. The same constraints as in previous simulation are enforced to controller. In this simulation, the heave disturbance is assumed to be predictable. The heave disturbance is given by $v_d = cos(2\pi t/12)[m]$, where $2\pi/12$ corresponds closely to the most dominant wave frequency in the North Atlantic, with reference to the JONSWAP spectrum [2], [19]. The input weight for MPC with future knowledge of heave disturbance is chosen $R = 85$. Figure 12 compares the responses of MPC controller without future knowledge of heave disturbance and

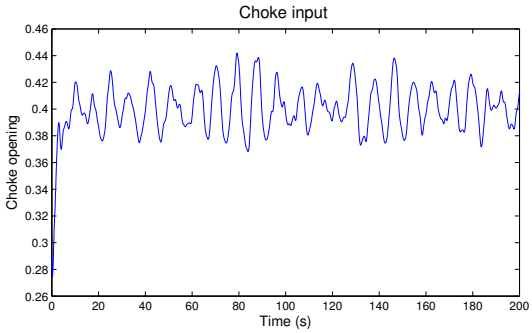

Figure 10. MPC control signal to the choke with heave disturbance.

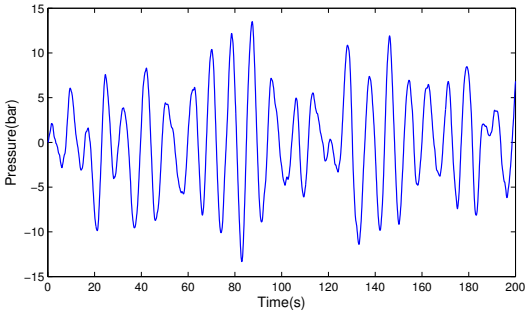

Figure 11. Heave disturbance

MPC with future knowledge of heave disturbance to track the set point reference. It is found that the MPC controller with future knowledge of heave disturbance reduces the effect of heave disturbance more than MPC controller without future knowledge of heave disturbance. This may motivate further research on short-term heave motion prediction based on forward-looking sensors such as ocean wave radar.

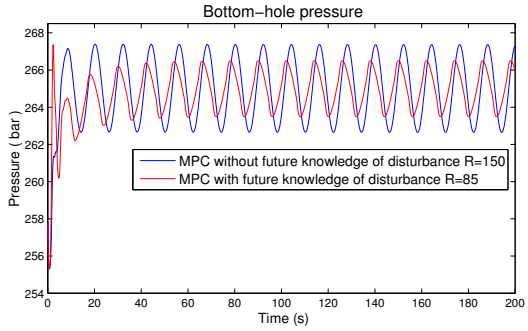

Figure 12. Bottom-hole pressure with predictable heave disturbance.

V. Conclusions

In this paper a dynamical model describing the flow and pressure in the annulus is used. The model was based on a hydraulic transmission line, and is discretized through a finite volumes method. A stochastic model describing sea waves in the North Sea was given.

A constrained MPC for controlling bottom hole pressure during oil well drilling was designed. It was found that

the constrained MPC scheme is able to successfully control the downhole pressure. It was also found that a constrained MPC shows improved attenuation of the heave disturbance. Comparing the PID controller results with MPC shows that the MPC controller has a better performance than the PID controller.

ACKNOWLEDGMENT

The authors gratefully acknowledge the financial support provided to this project through the Norwegian Research Council and Statoil ASA (NFR project 210432/E30 Intelligent Drilling).

REFERENCES

[1] I. S. Landet, H. Mahdianfar, U. J. F. Aarsnes, A. Pavlov, and O. M. Aamo, "Modeling for mpd operations with experimental validation," in *IADC/SPE Drilling Conference and Exhibition*, no. SPE-150461. San Diego, California: Society of Petroleum Engineers, March 2012.

[2] I. S. Landet, A. Pavlov, and O. M. Aamo, "Modeling and control of heave-induced pressure fluctuations in managed pressure drilling," *IEEE Transactions on Control Systems Technology*, 2013.

[3] J. Petersen, R. Rommetveit, K. S. Bjørkevoll, and J. Frøyen, "A general dynamic model for single and multi-phase flow operations during drilling, completion, well control and intervention," in *IADC/SPE Asia Pacific Drilling Technology Conference and Exhibition*, no. 114688-MS. Jakarta, Indonesia: Society of Petroleum Engineers, August 2008.

[4] H. Mahdianfar, A. Pavlov, and O. M. Aamo, "Joint unscented kalman filter for state and parameter estimation in managed pressure drilling," in *European Control Conference*. Zurich, Switzerland: IEEE, July 2013.

[5] G.-O. Kaasa, Ø. N. Stamnes, O. M. Aamo, and L. S. Imsland, "Simplified hydraulics model used for intelligent estimation of downhole pressure for a managed-pressure-drilling control system," *SPE Drilling and Completion*, vol. 27, no. 1, pp. 127–138, March 2012.

[6] G. Nygaard, L. Imsland, and E. A. Johannessen, "Using nmpc based on a low-order model for control pressure druing oil well drilling," in *8th International Symposium on Dynamics and Control of Process Systems*, vol. 8, no. 1. IFAC, 2007.

[7] Ø. Breyholtz, G. Nygaard, H. Siahaan, and M. Nikolaou, "Managed pressure drilling: A multi-level control approach," in *SPE Intelligent Energy Conference and Exhibition*, no. 128151-MS. Utrecht, The Netherlands: Society of Petroleum Engineers, March 2010.

[8] J. Zhou, Ø. N. Stamnes, O. M. Aamo, and G.-O. Kaasa, "Switched control for pressure regulation and kick attenuation in a managed pressure drilling system," *IEEE Transactions on Control Systems Technology*, vol. 19, no. 2, pp. 337–350, 2011.

[9] J. Zhou and G. Nygaard, "Automatic model-based control scheme for stabilizing pressure during dual-gradient drilling," *Journal of Process Control*, vol. 21, no. 8, pp. 1138–1147, September 2011.

[10] J.-M. Godhavn, A. Pavlov, G.-O. Kaasa, and N. L. Rolland, "Drilling seeking automatic control solutions," in *Proceedings of the 18th World Congress*, vol. 18, no. 1, The International Federation of Automatic Control. Milano, Italy: IFAC, September 2011, pp. 10 842–10 850.

[11] O. S. Rasmussen and S. Sangesland, "Evaluation of mpd methods for compensation of surge-and-swab pressures in floating drilling operations," no. 108346-MS, IADC/SPE Managed Pressure Drilling & Underbalanced Operations. Texas, U.S.A.: IADC/SPE, March 2007.

[12] A. Pavlov, G.-O. Kaasa, and L. Imsland, "Experimental disturbance rejection on a full-scale drilling rig," in *8th IFAC Symposium on Nonlinear Control Systems*. University of Bologna, Italy: IFAC, September 2010, pp. 1338–1343.

[13] H. Mahdianfar, O. M. Aamo, and A. Pavlov, "Attenuation of heave-induced pressure oscillations in offshore drilling systems," in *American Control Conference (ACC)*. Montréal, Canada: IEEE, June 2012, pp. 4915–4920.

[14] ——, "Suppression of heave-induced pressure fluctuations in mpd," in *Proceedings of the 2012 IFAC Workshop on Automatic Control in Offshore Oil and Gas Production*, vol. 1. Trondheim, Norway: IFAC, May 2012, pp. 239–244.

[15] D. Q. Mayne, J. B. Rawlings, and P. O. Rao, C. V.and Scokaert, "Constrained model predictive control: Stability and optimality," *AUTOMATICA*, vol. 36, no. 6, pp. 789–814, 2000.

[16] M. Morari and J. H. Lee, "Model predictive control: past, present and future," *AUTOMATICA*, vol. 23, no. 4-5, pp. 667–682, May 1999.

[17] C. E. García, D. M. Prett, and M. Morari, "Model predictive control: Theory and practice—a survey," *AUTOMATICA*, vol. 25, no. 3, p. 335˙348, May 1989.

[18] J. M. Maciejowski, *Predictive Control with Constraints*. Prentice Hall, 2002.

[19] I. S. Landet, A. Pavlov, O. M. Aamo, and H. Mahdianfar, "Control of heave-induced pressure fluctuations in managed pressure drilling," in *American Control Conference (ACC)*. Montréal, Canada: IEEE, June 2012, pp. 2270–2275.

[20] T. I. Fossen, *Handbook of Marine Craft Hydrodynamics and Motion Control*. John Wiley & Sons, April 2011.

[21] U. A. Korde, "Active heave compensation on drill-ships in irregular waves," *Ocean Engineering*, vol. 25, no. 7, pp. 541–561, July 1998.

[22] K. Do and J. Pan, "Nonlinear control of an active heave compensation system," *Ocean Engineering*, vol. 35, no. 5–6, pp. 558–571, April 2008.

[23] S. Kuchler, T. Mahl, J. Neupert, K. Schneider, and O. Sawodny, "Active control for an offshore crane using prediction of the vessel's motion," *IEEE/ASME Transactions on Mechatronics*, vol. 16, no. 2, pp. 297–309, April 2011.

[24] M. K. Ochi, *Ocean Waves - The Stochastic Approach*. Cambridge University Press, 2005.

[25] W. H. Michel, "Sea spectra revisited," *Marine Technology*, vol. 36, no. 4, pp. 211–227, 1999.